Urban hydrogeology

Transport routes and mixing of water and solutes in a groundwater influenced urban lowland catchment

Yu, Liang; Rozemeijer, Joachim C.; van der Velde, Ype; van Breukelen, Boris M.; Ouboter, Maarten; Broers, Hans Peter

DOI
10.1016/j.scitotenv.2019.04.428

Publication date
2019

Document Version
Final published version

Published in
Science of the Total Environment

Science of the Total Environment 678 (2019) 288–300

Contents lists available at ScienceDirect

Science of the Total Environment

journal homepage: www.elsevier.com/locate/scitotenv

Urban hydrogeology: Transport routes and mixing of water and solutes in a groundwater influenced urban lowland catchment

Liang Yu [a,b,c,*], Joachim C. Rozemeijer [d], Ype van der Velde [a], Boris M. van Breukelen [e], Maarten Ouboter [b], Hans Peter Broers [c]

[a] Faculty of Science, Vrije University Amsterdam, Amsterdam 1181HV, the Netherlands
[b] Waternet Water Authority, Amsterdam 1096 AC, the Netherlands
[c] TNO Geological Survey of the Netherlands, Utrecht 3584 CB, the Netherlands
[d] Deltares, Utrecht 3508 TC, the Netherlands
[e] Department of Water Management, Faculty of Civil Engineering and Geosciences, Delft University of Technology, Stevinweg 1, 2628 CN Delft, the Netherlands

HIGHLIGHTS

- Urbanization of lowlands changes mixing processes between the aqueous compartments.
- The impact of groundwater chemistry on surface water is strongest in dry seasons.
- Urban mixing changes hydrogeochemical reactions and retention patterns.
- Urban runoff brings oxygen and heavy metals to the water system.
- Residential deep water levels drive nutrient rich groundwater towards surface water.

GRAPHICAL ABSTRACT

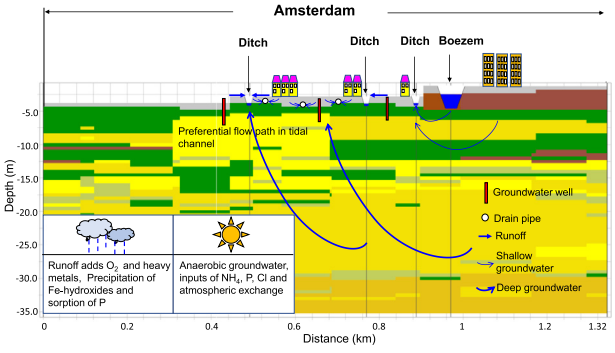

ARTICLE INFO

Article history:
Received 22 February 2019
Received in revised form 19 April 2019
Accepted 28 April 2019
Available online 29 April 2019

Editor: José Virgílio Cruz

Keywords:
Amsterdam
Surface water quality
Groundwater quality
Groundwater-surface water interaction
Radon
Nutrients

ABSTRACT

Urban areas in coastal lowlands host a significant part of the world's population. In these areas, cities have often expanded to unfavorable locations that have to be drained or where excess rain water and groundwater need to be pumped away in order to maintain dry feet for its citizens. As a result, groundwater seepage influences surface water quality in many of such urban lowland catchments. This study aims at identifying the flow routes and mixing processes that control surface water quality in the groundwater-influenced urban catchment Polder Geuzenveld, which is part of the city of Amsterdam. Geuzenveld is a highly paved urban area with a subsurface rain water collection system, a groundwater drainage system, and a main surface water system that receive runoff from pavement and roofs, shallow groundwater and direct groundwater seepage, respectively. We conducted a field survey and systematic monitoring to identify the spatial and temporal variations in water quality in runoff, ditch water, drain water, and shallow and deep groundwater. We found that Geuzenveld receives a substantial inflow of deep, O_2-depleted groundwater, which is enriched in ammonium and phosphorus due to the subsurface mineralization of organic matter under sulfate-reducing conditions. This groundwater is mixed in the ditches during wet periods with O_2-rich runoff, and iron- and phosphate-rich drain water. Unlike natural catchments, the newly created, separated urban flow routes lead to mixing of water in the main surface water itself, shortcutting much of the soil and shallow subsurface. This leads to low O_2 and high ammonia concentrations in dry periods, which might be mitigated by water level management or artificially increasing O_2 levels by water inlet or

* Corresponding author at: Faculty of Science, Vrije University Amsterdam, Amsterdam 1181HV, the Netherlands.
E-mail address: l.yu@vu.nl (L. Yu).

https://doi.org/10.1016/j.scitotenv.2019.04.428

artificially aeration of the main water canals. Further research is necessary how to optimize artificial urban systems to deliver a better ecological and chemical status of the surface water.

1. Introduction

As cities expand worldwide, the urban natural water resources are under stress of contamination, and ecological degradation by human activities (Leopold, 1968; McPherson, 1974; Paul and Meyer, 2001; Foster, 2001; Walsh et al., 2005; Pataki et al., 2011; Gumindoga et al., 2014). Meanwhile, urban waters are increasingly used for recreation such as boating, swimming, waterside picnics, etc. Urbanization involves modifications in the natural water cycle by the introduction of impermeable surfaces and the installation of urban drainage systems. These modifications reduce infiltration, increase urban runoff, and may shorten the hydrological travel times. In addition, urbanization often involves the contamination of shallow groundwater and surface water with for example nutrients and heavy metals. The degeneration of urban water quality initiated interest in research on concentrations, sources, and sinks of pollutants in cities (e.g. Hall and Ellis, 1985; Gobel et al., 2007; Howard and Maier, 2007; Boogaard et al., 2014; Kojima et al., 2017; Zafra et al., 2017; Hobbie et al., 2017; Yang and Toor, 2018, etc.). Typical urban pollutants include heavy metals, nutrients, and organic contaminants. In many cases the urban water systems are relatively simple: rain via runoff brings heavy metals generated by traffic, roofs, and other construction materials into the surface water system. Urban fertilizer application, waste water inflow, and atmospheric deposition introduce nutrients which are transported by superficial pathways (D.R. Oros et al., 2007; Nyenje et al., 2010; Berndtsson, 2014). However, these pollutants may also infiltrate, causing groundwater pollution (Morris et al., 2006a, 2006b; Sorensen et al., 2015; Bonneau et al., 2017; Abdalla and Khalil, 2018) and a delayed response of surface water quality downstream. Most urban groundwater research is typically emphasizing the deep infiltration of recent anthropogenic substances and on tracing the origin and age of the infiltrated water (e.g. Morris et al., 2006a, 2006b). Expanding cities in lowland areas are differently affected by groundwater, as surface water quality might be significantly influenced by upward groundwater seepage (Ellis and Rivett, 2007; Gabor et al., 2017). In a previous study (Yu et al., 2018), upward seeping polders in the greater area of Amsterdam were shown to transport relatively high nutrients fluxes to the main water system, but these polders were never investigated in detail.

To create more space for residential areas, low-lying natural wetlands, lakes, and excavated peat areas around Amsterdam have been reclaimed and urbanized. Large amounts of excessive water are being pumped out every day to maintain low surface and groundwater levels and prevent wet cellars or flooding of residential areas. The surface water levels, groundwater levels, and flow routes are regulated by pumping schemes. Factors like the electricity price, the choice of vegetation, maintenance frequencies, and city constructions including the drainage system design all influence the hydrology and water quality in such areas. Since the potentially eutrophicated and degraded surface waters gained more attention because of European legislation, such as the Water Framework Directive (EC, 2000), researchers and governments noticed that the urban routes of pollutants have not been considered enough, which creates a potential barrier for an effective mitigation of urban water quality problems.

Little research has been carried out in lowland groundwater-fed urban catchments. Therefore, little is known about the flow routes of nutrients and other chemical variables from the subsurface of a city, which are an indirect consequence of the human manipulation of the hydrology. In addition, there is a lack of knowledge of the geochemical processes during the mixing of upwelling groundwater with rain water in the surface water system. Some studies addressed the mixing of water sources in urban settings in process-based models (e.g. Yan et al., 2018), but good measurement datasets for validation are lacking. As lowland cities are rapidly expanding worldwide, more wetlands will change into low-lying, groundwater-fed, artificial urban catchments. Understanding sources and flow routes of water and solutes and potential reaction processes is key to improve the water quality conditions in urban lowland settings.

The objectives of this study are to (1) identify the flow routes of nutrients, heavy metals, and major ions in a groundwater-influenced urban catchment, (2) to interpret the mixing of the runoff, drain water and groundwater in the surface water system through space and time, and (3) to formulate hypotheses on the effects of city infrastructure on urban water quality as a basis for further research. To address these goals, a spatial survey of the polder water system was performed and time series of water quality parameters and natural tracers (^{222}Rn and δ^{13}C-DIC) were collected for 8 locations during 2016–2017 at weekly and biweekly intervals, and a longer time series was collected at the pumping station during 2006–2016 at monthly intervals. We interpreted the time series data applying a temporal water quality separation based on APEI (Antecedent Precipitation and Evaporation Index), as the contribution of different flow routes depends on the meteorological and hydrological conditions (Rozemeijer and Broers, 2007). Empirical and statistical methods were applied to interpret the flow routes and mixing of water within the polder system.

2. Methods

2.1. Study site

The urban polder Geuzenveld is located in the western part of the city of Amsterdam (Fig. 1). Its urban surface area covers 0.47 km^2, including a small park in the south. The area has a population of 2430 and its average elevation is 2.75 m below the Normaal Amsterdams Peil (NAP: Normalized Amsterdam Peil, a known standard conforming to mean sea level). The polder is the result of the excavation of peat in the early 20th century and the resulting lake was reclaimed between 1937 and 1941. Originally, the polder was in agricultural use, but between 1990 and 2000 the polder was converted to a residential area. The water levels in the urban polder and the park are maintained at 4.25 m below NAP. Open water area occupies 7% of the total urban area. There are three ditches in North-South direction (called West ditch, Middle ditch, and East ditch) and two in West-East direction. The East ditch is the narrowest with <1 meter width and <0.5 m in depth in general (Fig. 1, E1 and E2), the other ditches have widths ranging from 2 to 5 m and are about 1 to 1.5 m deep. At least 50% of the polder is covered by houses and other impermeable or semi-permeable land surfaces such as concrete brick stones and asphalt streets. Around 25% of the area is unpaved, consisting of the park in the south, public and private gardens and small unpaved strips along the streets.

The average annual rainfall in the Amsterdam area is about 847 mm/year and the average annual evaporation (Makkink, 1957) is approximately 609 mm/year (2006–2017 average calculated from KNMI Schiphol meteo station in Amsterdam, http://www.knmi.nl). Because of the substantial groundwater seepage (estimated rate 0.6 mm/day) input to the Geuzenveld surface water system, water inlet during dry periods is not needed to maintain the water levels. The surplus water is pumped out by the pumping station in the northeast corner towards, the so-called “Boezem-system” (waterways that have a higher water level, see also Yu et al., 2018) which is annotated with B and B′ in Fig. 1.

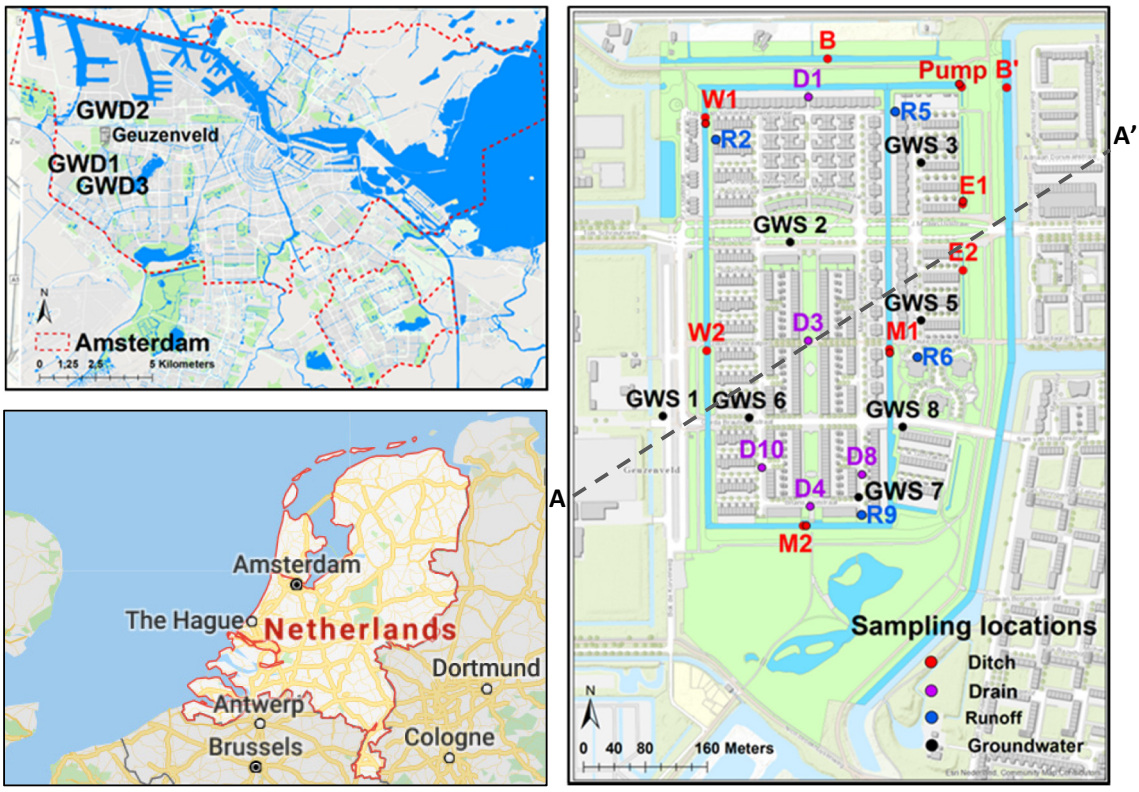

Fig. 1. Location of polder Geuzenveld (52°23′01.3″N 4°47′37.7″E) in the greater Amsterdam area (left figure) and detailed map of Geuzenveld (right figure). The Amsterdam map shows the location of polder Geuzenveld and the deep groundwater sampling locations (GWD1, GWD2 and GWD3). The Geuzenveld map shows the sampling locations of the short term (2016–2017) grab sampling (W1, W2, M1, M2, E1, E2, B, and B′), the water quality survey in 2017 of runoff (R2, R5, R6, and R9), ditch (W1, M1, M2, E1, and Pump) and drain water sampling manholes (D1, D3, D4, D8, D10) and shallow groundwater piezometers (GWS 1–3, GWS 5–8).

Being a young urban polder built in 1990s (Fig. 1), Geuzenveld has a relatively modern separated drainage system. The drainage system includes a rain water drainage system, a groundwater drainage system, and a sewer system (Fig. 2, and SI-Figs. SI 1.1, 1.2 and 1.3). A rainwater collection system is installed on all the houses which either leads rain water towards manholes and further to the ditches, or directly to the ditches. The groundwater drainage system consists of perforated pipes mostly at a depth of approximately 2 m below the surface. It collects both rainwater that infiltrates in the non-paved areas and shallow groundwater. The drains have a direct connection to the ditches. During low discharge periods a return flow from the ditches into the rain and drain pipes and manholes was observed. The sewer system separately transports household waste water towards a sewage treatment plant outside the polder and is disconnected from the polder water system. Potential leakage of sewerage into the subsurface cannot be completely excluded, but we found no evidence for this.

The subsurface deeper than 30 m below NAP is made up of a buried ice-pushed ridge of Pleistocene age formed by the Saalien land ice mass (Schokker et al., 2015; Fig. 2). The coarse sand deposits of the covered ice-pushed ridge are overlain by fluvial sandy deposits of the Rhine river (KRBXDE) and aeolian deposits of the Late Pleistocene (Boxtel Formation: BX). This sequence of Pleistocene deposits forms the main aquifer in this area. The aquifer is overlain by Holocene deposits of marine and peri-marine environments. The Holocene cover layer mainly consists of clays and clayey sands of the Wormer Member of the Naaldwijk Formation (green in Fig. 2) that were deposited in a tidal flat environment. Two peat layers are prominent in the western part of the Netherlands. The basal peat (NIBA) is typically at the basis of the Holocene sequence. This peat layer is typically strongly compacted and is known to represent a hydraulic barrier in the western part of the Netherlands (Stafleu et al., 2011). The second peat layer rests on top of the Holocene clays of the Naaldwijk Formation (NIHO). This shallower peat layer was excavated in the 20th century in this polder which was part of a larger polder called “The Eendracht” at that time. The peat is still existent in the urban area just east of the polder and in the North (see east side of Fig. 2). This “Holland Peat” (NIHO) is also present directly east of the deep polder, where it forms the base of the waterway with the highest water levels in the residential area east of the polder and forms the dike between the two areas. In the southwest of the polder the clays of the Naaldwijk Formations were removed by erosion by a tidal channel from the Zuiderzee-IJ-estuary that deposited moderately fine to very fine sands (Fig. 2: channel deposits in blue, Schokker et al., 2015). The urban area is part of the marginal area of the former Zuiderzee estuary as described in Yu et al. (2018) who described the groundwater and surface water quality of the larger Amsterdam region. The brackish influence of the former Zuiderzee is still reflected in the presence of brackish groundwater and seepage of brackish groundwater in both urban and agricultural polder catchments (e.g. Delsman et al., 2014).

On top of the geological deposits an artificial anthropogenic layer was created for developing the urban quarter (AAOP in Fig. 2). It consists of an approximately one-meter thick sand layer that was supplied over the existing clayey polder surface. This artificial layer promotes the drainage of groundwater and rain water to a system of collection drains, thus keeping groundwater levels low enough to avoid water inconveniences in the urban settings. Fig. 2 shows the position of these drains and the water levels that are maintained in the urban quarter (for details, see to SI-Figs. SI 1.1–1.3).

2.2. Data collection

To identify the flow routes of solutes and the mixing of different water sources within the polder system, water quality data were collected covering both the spatial patterns and temporal variations. We

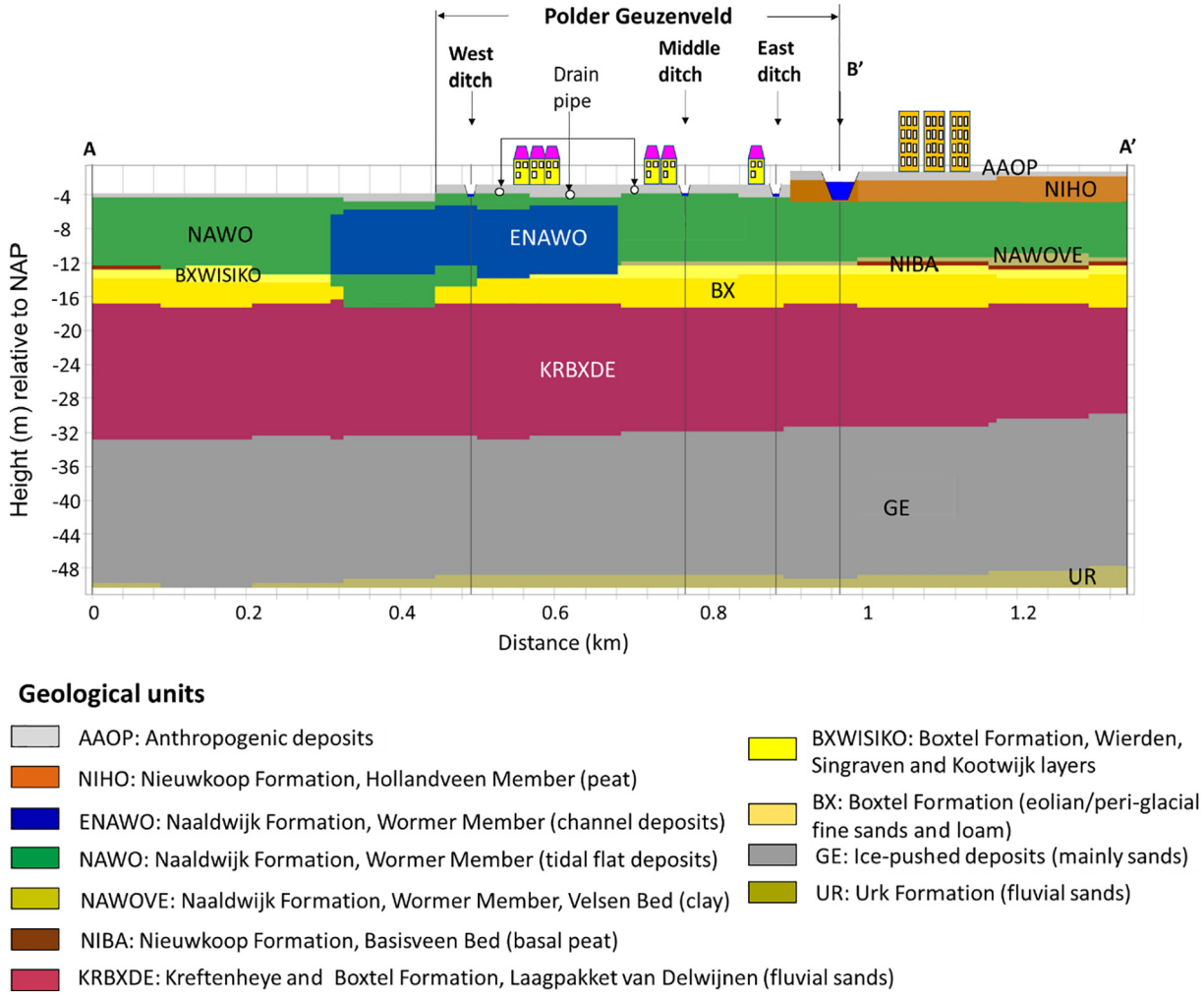

Fig. 2. Geological Formations and their main lithology beneath the polder Geuzenveld with indicative positions of the main water courses and drains. A more detailed lithology based on 100 × 100 × 0.5 m voxels (Schokker et al., 2015) for this cross-section is given in Fig. 8. The cross-section A–A′ is indicated in Fig. 1.

profited from the long-term time series of water quality monitoring by the Waternet water board covering the period 2006–2017. We intensified the monitoring through higher frequency grab sampling during 2016–2017, a groundwater water quality investigation from 2017-05-28 to 2017-05-30, spatial surveys of individual flow routes from 2017-11-28 to 2017-12-01, and groundwater tracer measurements (δ^{13}C-DIC and ^{222}Rn).

2.2.1. Runoff, ditch, drain, and groundwater water sampling

A first investigation of deep (GWD) and shallow (GWS) groundwater quality was conducted from 2017-05-28 to 2017-05-30, including 9 piezometers (GWS 1–3, GWS 5–8 and GWD 1–2, Fig. 1). Groundwater sampling of the shallow piezometers with 1 meter length screens up to 5 meter depth (GWS) concentrated on the polder Geuzenveld itself, whereas the deeper groundwater was sampled for two piezometers at 10 to 25 meter depths with screen lengths of 1 m at about 2 km distance from our urban study polder Geuzenveld. An extra spatial survey was carried out from 2017-11-28 to 2017-12-01, in order to distinguish between the different flow routes that influence ditch water quality. The survey was carried out in a period with ample rain (cumulative 17.2 mm in the two days preceding the sampling from 2017-11-26 10:00 until 2017-11-28-10:00 (SI-Fig. SI 8.1)) when drain and rain water systems discharged significant amounts of water. The survey included (Fig. 1): (1) the sampling of runoff from the rain water system (Rain: R2, R5, R6 mix (runoff from the roof and the street), R6 street (runoff from the street), and R9), (2) the ditch water at locations West 1 (W1), Middle 1 (M1), Middle 2 (M2), East 1 (E1), and the pumping station (Pump), (3) the effluents of the artificial groundwater drainage system (Drains: D1, D3, D4, D8 and D10) and (4) the shallow and deep groundwater from piezometers (GWS 1–3, GWS 5–8 and GWD 1–3). Drain water and runoff samples were collected from manholes that allowed access to these water flow paths (SI-Figs. SI 1.1–1.3). Parameters measured in the spatial survey included pH, O_2, EC, Temperature, HCO_3, Cl, SO_4, Na, Ca, K, Mg, Fe, Mn, NH_4, NO_3, TP, DOC, Ba, Sr, Ni, Al, Pb, As, Cd, Cr, Cu, and Zn.

2.2.2. Long and short term surface water quality monitoring (2006–2017 and 2016–2017)

A low frequency (monthly) time series of water quality from grab sampling was collected by Waternet from 2006 to 2017 following the procedures used by the Dutch water boards. The monthly sampling was done at the location in front of the pumping station ("Pump" in Fig. 1). A higher frequency (weekly and biweekly) grab sampling campaign was carried out between 2016-03-14 and 2017-06-16. Samples were mostly taken in the center of the canals both laterally and vertically. Sampling at the pumping station (Pump) conformed with the low frequency sampling of the previous years but at higher (weekly and biweekly) frequency. Additional samples were collected from 8 other locations in the polder, West 1 (W1), West 2 (W2), Middle 1 (M1), Middle 2 (M2), East 1 (E1), East 2 (E2), and Boezem (B and B′)

(see Fig. 1). Here, locations M1, M2, W1 and W2 represent the main ditches in the polder system that collect water from all the drainage systems present (runoff and drain water and groundwater seepage). Ditches E1 and E2 have smaller dimensions and mainly drain the foot of a dike at the east part of the polder, and do not receive water from runoff or drains.

2.2.3. δ^{13}C-DIC and ^{222}Rn sampling

δ^{13}C-DIC was measured as an additional parameter at three selected locations (M2, E2 and B′), as we hypothesized that the δ^{13}C-DIC values would differ between the end members of our mixed surface water samples. We expected δ^{13}C-DIC of groundwater to be mainly determined by organic matter mineralization (δ^{13}C-DIC $= \pm -25‰$ of C3 plants) and the dissolution of subsurface calcite (δ^{13}C-DIC 0‰) yielding values around −12‰ to be significantly different from runoff which is believed to be in equilibrium with atmospheric CO_2 (e.g. Mook, 2006; δ^{13}C-DIC $= \pm -8‰$). To trace groundwater inflow, ^{222}Rn activity was additionally measured at all locations (Fig. 3). ^{222}Rn is a radioactive gas that is produced by the decay of ^{226}Ra from the radioactive decay of uranium and is often used as a tracer for groundwater inflow into surface water (e.g. Cecil and Green, 2000; Dimova et al., 2013; Cartwright and Hofmann, 2016). Groundwater concentrations of ^{222}Rn are typically much higher than in receiving surface waters because of the continuous decay of ^{226}Ra which is present in minerals or adsorbed at reactive phases in the aquifer matrix. The radon gas is released continuously from subsurface minerals that contain ^{226}Ra and is mildly soluble in water. ^{222}Rn has a half-life of 3.8 days, which makes it suitable for tracing the very recent groundwater input into surface water bodies, although the method has drawbacks because the degassing of ^{222}Rn to the atmosphere is a process that is heavily dependent on the specific field and weather conditions (Cartwright and Hofmann, 2016).

2.3. Data processing

The field sampling campaigns yielded three datasets for processing: (1) the 2017 spatial survey dataset consists of a single water quality survey for runoff, ditch water, drain water, and groundwater at 24 locations; (2) the 2016–2017 time series at 8 locations with weekly/bi-

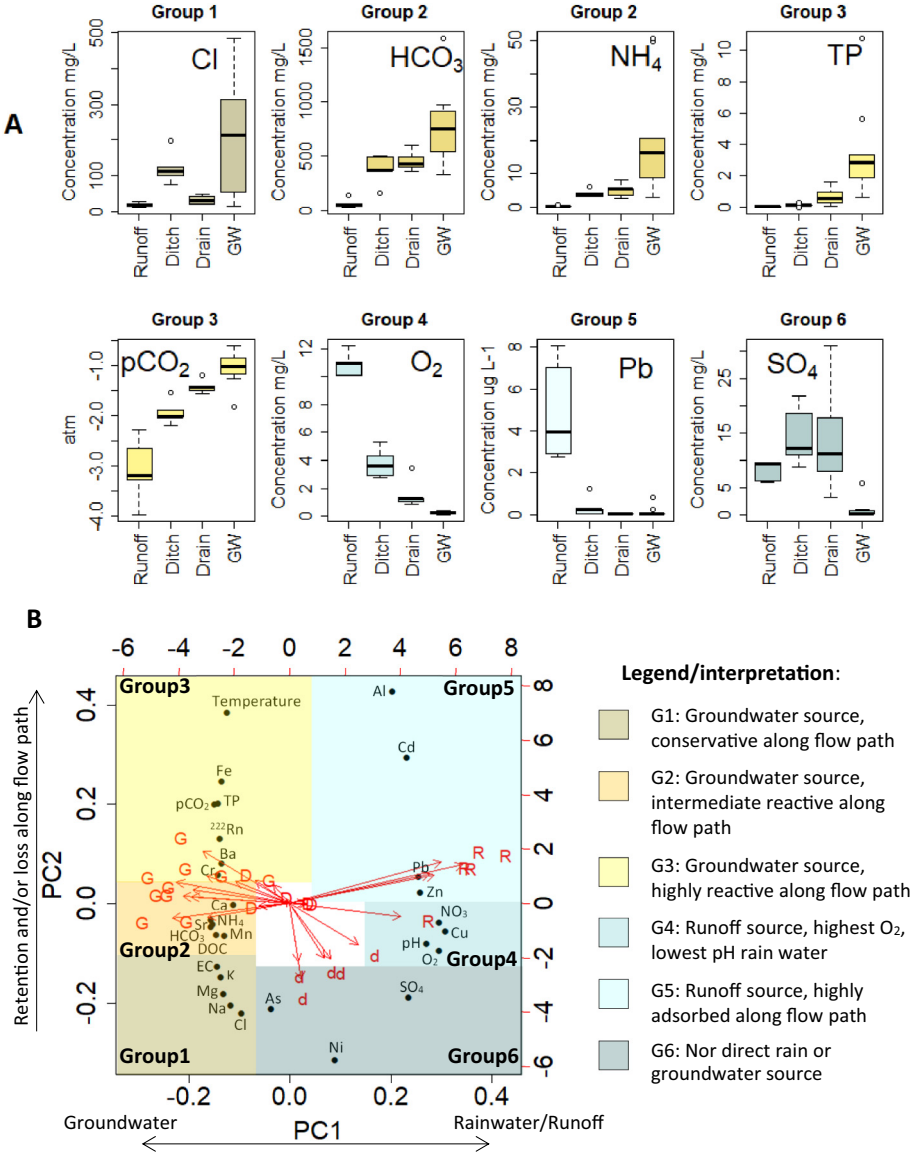

Fig. 3. Results of the PCA analysis in graphical form. Panel A: Boxplots of the concentrations of flow route indicators based on the PCA analysis of the data collected during the 2017 spatial survey. PC1 and PC2 explain 76% of the variance. Boxplots for the complete set of solutes are given in SI 2 Fig. SI 2.1. At least one solute from each group in the PCA results of panel B is shown. Panel B shows the contributions of the first 2 principle components (PC1 and PC2) to explain the observed solute concentrations. The arrows in panel B indicate the loadings of the flow routes sampled: runoff (R, observation number n = 5), ditch water (d, n = 5), drain water (D, n = 5), and groundwater (G, n = 10).

weekly sampling; and (3) the 2006–2017 long time series with monthly data at the pumping station.

The water quality data of runoff, ditch water, drain water, and groundwater were summarized in a group of boxplots. We applied Principal Component Analysis (PCA) to the 2017 Survey dataset, to identify solutes with similar behavior along the flow routes and the major controls on chemical composition of the waters within the polder. Because many of the water quality parameters were not normally distributed, and concentrations between parameters differ strongly, we normalized (via a box-cox transformation) and scaled all the variables. By plotting the first two principle components of the PCA, the water quality parameters were grouped into solutes with similar patterns along the flow routes.

For the interpretation of the temporal variations in water chemistry, we applied an Antecedent Precipitation and Evaporation Index (APEI) based on meteorological data to distinguish between periods with wet and dry conditions in the catchment (for details see SI 3). We divided the hydrological condition of the catchment for each day into 4 classes from driest (class 1) to wettest (class 4) based on the calculated APEI values as below, following the procedure of Rozemeijer et al., 2010:

$$APEI_t = APEI_{t-1} \times Decay\ rate + (Precipitation - Evaporation)_t \quad (2)$$

$APEI_t$ is APEI (mm) at day t.

The one-year surface water quality data (^{222}Rn, pCO_2, HCO_3, Cl, and Fe) of the 8 locations from 2016 to 2017 which fell in classes APEI = 1 (dry, see Section 3.2) to APEI = 4 (wet), were plotted with the runoff, ditch, drain, and groundwater data from the survey in 2017. The survey was intentionally done during a wet period (APEI class 4) in order to have all transport routes contributing during the survey. We used the survey results as reference for interpreting the transport routes during a wet period, comparing it with the data from the longer time series. In addition, the 2006–2017 and 2016–2017 time series of surface water concentrations measured at the pumping station were jointly summarized in boxplots for each of the 4 APEI classes.

3. Results & discussion

3.1. Runoff, ditch water, drain water, and groundwater flow routes survey

The November 2017 survey yielded a dataset of 27 water quality parameters on 24 locations that span the dominant flow routes in our catchment: runoff (4 locations), drain water (5 locations), ditch water (5 locations), and shallow and deep groundwater (10 locations). A PCA on this dataset returned 2 principle components that explain 76% of the total variance (Fig. 3). Based on these first 2 principle components, we grouped the 27 water quality parameters into 6 groups with similar flow route concentration patterns (Fig. 3).

Groups 1–3 contain the solutes that have the highest concentrations in groundwater but the lowest in runoff (Fe, Temperature, pCO_2, TP, ^{222}Rn, Ba, Cr, NH_4, Ca, Sr, HCO_3, DOC, Mn, Cl, EC, K, Mg, and Na). Groups 4 and 5 have the highest concentrations in runoff (Al, Cd, Pb, Zn, Cu, NO_3, pH and O_2). Group 6 contains three solutes that have the highest concentrations in drains and/or ditches (As, Ni, SO_4).

The solutes that were highest in groundwater (Groups 1–3) were further subdivided into three groups with each a characteristic flow route pattern (see Fig. 3 boxplots):

- Group 1: concentrations in ditches are significantly higher than in drains (Cl, EC, K, Mg, and Na),
- Group 2: concentrations in ditches are similar to that of the drains (NH_4, Ca, Sr, HCO_3, DOC, and Mn),
- Group 3: concentrations in drains are significantly higher than those of the ditches (Fe, Temperature, pCO_2, TP, ^{222}Rn, Ba, Cr).

Similarly, the solutes with highest concentrations in runoff were also divided into 2 groups:

- Group 4: ditch concentrations clearly higher than the drain concentrations (O_2, pH, NO_3, Cu),
- Group 5: both ditch and drain concentrations are similar and much lower than in runoff (Pb, Zn, Cd, Al).

The median concentrations of As, Ni, and SO_4 (Group 6) were highest in the ditches and drains as opposed to groundwater and runoff, which distinguishes these variables from the rest. Although Ni and As are attributed to this group, the patterns of Ni and As also conforms to some extent with group 2 (NH_4, Ca, Sr, HCO_3, DOC, and Mn).

Characteristic examples of each of these groups are given in Fig. 3, all solutes are presented in SI 2 Fig. SI 2.1.

The PCA confirms our hypothesis that groundwater and runoff are the two dominant sources of solutes in polder Geuzenveld (opposite directions of the G and R arrows along the principle component 1 (x-axis) representing the loadings of each of these flow routes, Fig. 3 B). We derive the following conclusions from the PCA:

- The groundwater is characterized by a neutral pH (6.8–7.0) resulting from carbonate mineral dissolution (as indicated by Ca, HCO_3 and pCO_2), reduced conditions (low $O_2 < 0.5$ mg/L), nutrients enrichment (TP and NH_4), and a seawater influence (high Cl, Na, K and Mg). The reduced conditions allow Mn and Fe to be present in their reduced soluble form (Fe^{2+}, Mn^{2+}) (Appelo and Postma, 2010).
- The runoff is O_2-rich and contains heavy metals that are presumably desorbed and dissolved from roofs and paved areas (R arrows in Fig. 3B).
- Drains (arrows with D's in Fig. 3B) discharge the shallow groundwater, which consists of a mixture of groundwater and infiltration from rain in unpaved and partially paved terrains.
- In the main receiving ditches, waters from these three flow routes (groundwater, rain water and drain water) mix and react with each other (d arrows in Fig. 3B).

The first principle component (PC1) of the PCA analysis clearly reflects the mixing of groundwater with runoff, where solutes that originate from groundwater are plotted at the left side and solutes that originate from runoff at the right. The mixing process of these main origins is the major control on the solute composition of the water samples, explaining 66% of the total variance. We interpret the second principle component (PC2) of the PCA, which explains another 10% of the total variance, to reflect the reactivity of the solutes along the flow route from its source (groundwater or runoff) towards the ditch and further towards the pumping station. Here, Cl is being the least reactive (bottom part) and Fe and Al are the most reactive (upper part of the graph).

3.1.1. The groundwater derived solutes

Following the interpretation of PC2, the groups 1–3 represent solutes originating from groundwater that react along their flow route. Due to seawater influence, deep groundwater is relatively high in Cl, Na, Mg, and K and accordingly has an elevated EC (see also Yu et al., 2018 for a regional analysis of water types in the larger Amsterdam region). The higher concentrations of these stable solutes in the ditches compared with the drains point to the importance of direct flow paths of deep groundwater into the open water system. We interpret the similar concentration levels in the ditch and drains of solutes in group 2 to reflect moderate reactivity of these groundwater derived solutes under oxygenated conditions in drains and ditches. This reactivity intensifies going from drains to ditch due to both higher oxygen concentration and longer residence times in the ditch, which could explain the lower

ditch concentration relative to drain concentration of group 2 compared to group 1. Strong reactivity under oxygenated conditions in the ditch is found for the solutes in group 3; the reactivity of Fe and TP is suggested to be related to the precipitation of Fe-hydroxides following oxygen inflush from runoff with subsequent sorption of phosphorus, and to the exchange with the atmosphere (pCO_2 and ^{222}Rn) combined with radioactive decay for ^{222}Rn (see Section 3.3).

In a previous paper (Yu et al., 2018), we argued that high TP and NH_4 concentrations of the groundwater around Amsterdam are related to SO_4-reducing or even methanogenic conditions in the principal aquifers. The presence of reactive organic matter in the subsurface depletes the groundwater from oxygen and nitrate, leading to an overall low redox potential in groundwater, which enables the further decomposition of organic matter. Sulfate reduction is identified in our previous paper (Yu et al., 2018) as the dominant reaction causing organic matter oxidation in the study area. In the process of organic matter decomposition/mineralization, N and P are released in the form of dissolved and particle forms. The sulfate-reducing conditions led to increased HCO_3 concentrations and explain the presence of NH_4, HCO_3, and DOC, in the same group, group 2. However, TP that also originates from these nutrient-rich groundwaters, ends up in group 3 as it is much more reactive when the water is mixed with oxygenated water and Fe-hydroxides form that are able to sorb most of the phosphorus (Van der Grift et al., 2014, 2018). This is illustrated in Fig. 4 that shows that phosphorus in the ditches and the drains adjacent to the ditches (D1, D4), where oxygen from runoff is mixed with the groundwater and drain water, is mainly in the form of sorbed P (unfiltered P higher than filtered P). In contrast, phosphorus in groundwater and drain locations not affected by runoff (D3, D8, D10) is mainly in the form of dissolved ortho-P as

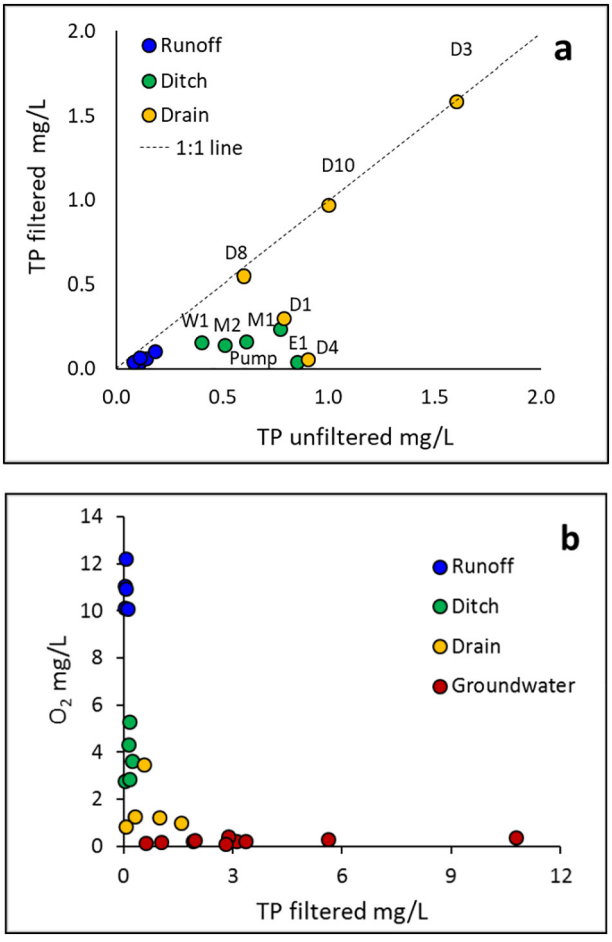

Fig. 4. Comparison of TP from filtered and unfiltered samples (a) and TP variation with O_2 (b).

this reduced water carries Fe(II) as main dissolved iron species under the low oxygen conditions encountered there. We suggest that the process of capturing of phosphorus in Fe-hydroxide particles in the transition zones between anoxic groundwater to oxic surface water, as was previously described by Van der Grift et al. (2014, 2018), determines the presence of Fe and TP in group 3 of the PCA analysis.

3.1.2. The runoff derived solutes

We interpret the difference between groups 4 and 5 as a result of a much higher retention of the heavy metals along the flow path from runoff, drain, to ditch (group 5) compared to the reactions that O_2, pH and NO_3 undergo along this same flow path (group 4). The high pH of urban runoff was somewhat surprising given the low pH of urban rain water, but can be explained by buffering of street water in contact with concrete building and pavement materials (Galan et al., 2010; Van der Sloot et al., 2011; Van Mourik et al., 2003). The enrichment of urban runoff with metals is in accordance with previous studies in urban areas, for example Berndtsson (2014) who concluded that Pb, Zn, Cu, Ni, and Cd in storm runoff are mostly bound to particles. Zn is a known contaminant to be released from zinc applied in roofs and rain collection systems and a constituent of car tyres, and both Zn and Pb are known to be associated with urban traffic (Smolders and Degryse, 2002; Gobel et al., 2007).

Group 6 grouped Ni, SO_4, and As. Especially Ni and sulfate stand out, as they showed the highest concentration in drain water and ditch water, meaning that direct groundwater seepage of sulfate and nickel does not occur in our polder. We hypothesize that oxygenated water that recharged under the parks, gardens, and other non-paved areas mixes with reduced shallow groundwater while converging towards the drain system. As the shallow subsoil of the polder catchment partly consist of a layer of supplied sand on top of a Holocene clay layer, we expect that the low groundwater levels and the oxygenated recharge water enable the oxidation of pyrite in the clay which mobilizes SO_4, Ni, and possibly As, which also has high concentration levels in groundwater (e.g. Dent and Pons, 1995; Zhang et al., 2009). As the groundwater is typically low in sulfate because of sulfate reduction (see Yu et al., 2018), we conclude that the drains are the main transport route for sulfate in our catchment.

3.2. Spatial and temporal variations in the urban catchment

3.2.1. Spatial variations in ditch water quality over wet and dry conditions

To further understand the functioning of our urban catchment under different weather conditions, we assessed the spatial and temporal variations of a number of water quality parameters over our March 2016–June 2017 sampling campaign. For this aim, we divided our samples based on the APEI at the moment of sampling, yielding four APEI classes ranging from dry to wet catchment conditions (see SI 3 for details). Fig. 5 summarizes the time series data for the wetness classes dry (APEI 1) and wet (APEI 4) and compares the monitoring data with the spatial survey data that were described in the previous section. The samples of the West (W), Middle (M), and East (E) were taken from the main ditches that collect the water in the urban polder, combining the W1 and W2, M1 and M2, and E1 and E2 measurements in order thus avoiding redundancy in the data. A mixture of water from those locations W, M and E is eventually pumped out at the main outlet (Pump) and pumped into the regional channel system (called "Boezem"), where location Boezem B′ was sampled. Because location B′ appeared to be directly influenced by the discharge from the pump, we chose Location B for "Boezem" water, using it as an independent reference to the measurement points in the polder itself.

The water quality variables in the polder ditches W, M, and E all reveal relatively low variability under dry conditions (APEI = 1) which is reflected in the low variability of the water composition that is pumped out of the polder at location P under these conditions. The anions HCO_3 (600–700 mg/L) and Cl (150–200 mg/L) dominate over SO_4 (<40 mg/L)

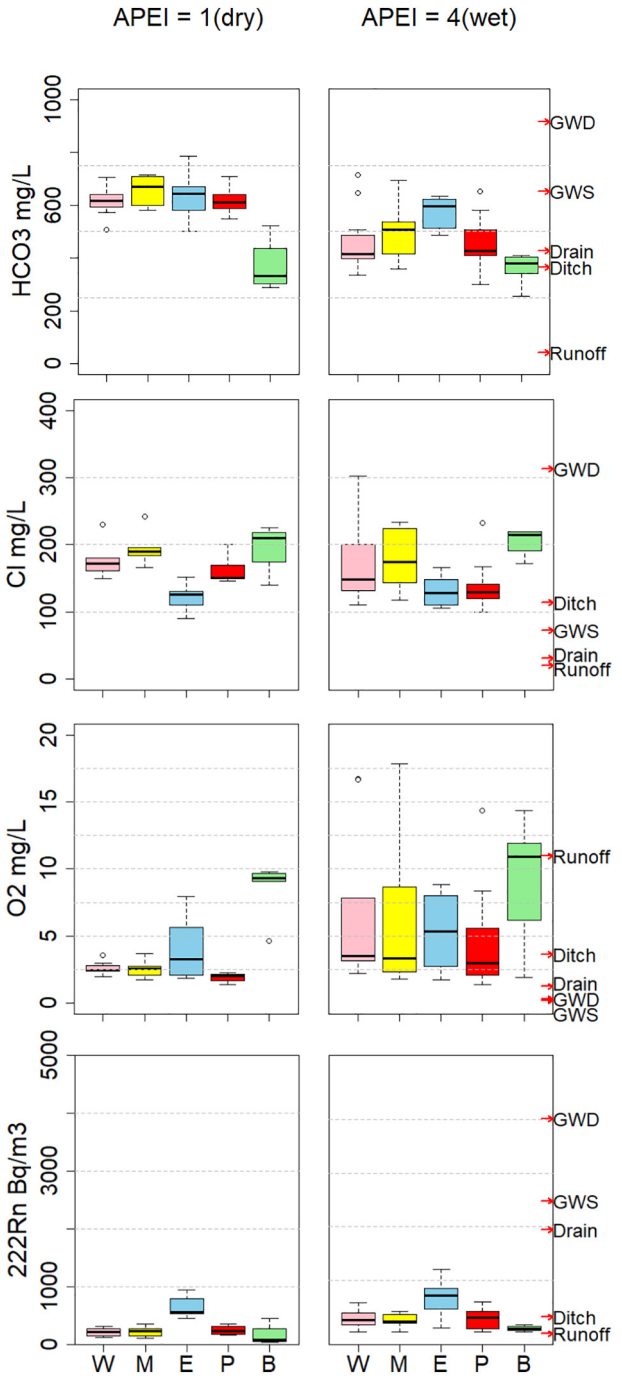

Fig. 5. Summary of the measured HCO_3, Cl, O_2, ^{222}Rn, and pCO_2 concentrations in the surface water aggregating the 2016–2017 data for dry periods (APEI class = 1) and wet periods (APEI class = 4). The locations of W, M, E, and B represent the total of measurements in the West ditch, the Middle ditch, the East ditch and boezem water north of Geuzenveld, respectively. "P" represents the measurements at the pumping station. Red arrows are used to illustrate the median concentrations that were observed in the 2017 spatial survey (see Section 3.1 and Fig. 3). GWD: deep groundwater, GWS: shallow groundwater, Drain: drain water, Ditch: ditch water, Runoff: rain water.

and NO_3 (<5 mg/L) (not shown). During these dry conditions, the water is characterized by high partial CO_2 pressure (~10^{-2} atm) and low, but constant O_2 concentrations (<3 mg/L). Variability increases for all variables under wet conditions (APEI = 4). Lower concentrations of Cl and HCO_3 are more typical, and the overall concentrations pumped out at location P decrease relatively to dry conditions. On the contrary, O_2 concentrations are much higher and range between 3 and 9 mg/L at most locations in the polder under wet conditions. The patterns for ^{222}Rn and pCO_2 do not change much, except that the variability tends to increase relative to dry conditions.

Relative to the locations W, M and P, the shallow ditches that drain the area near the eastern dike (E) exhibit lower Cl concentrations (100–150 mg/L), higher ^{222}Rn (600–800 Bq/m^3) and higher pCO_2 ($10^{-1.7}$–$10^{-1.2}$). These figures point to another origin of the seeping groundwater; especially the high ^{222}Rn is an indication that the seeping water at the foot of the dike was in direct contact with the subsurface and is replaced before concentrations are lowered by atmospheric exchange and the radioactive decay of the radon gas. Moreover, these shallow ditches are not connected to the runoff or drain system and do not show the variability that is introduced by diluting runoff or drain water under wet conditions.

The boezem water at B, which is not connected to the polder, shows a totally different chemistry, with much lower HCO_3 (300–400 mg/L), and partial CO_2 pressure ($10^{-2.8}$–$10^{-3.5}$ atm) and much higher O_2 (~10 mg/L). Both O_2 (~10 mg/L) and CO_2 (pCO_2 $10^{-2.8}$–$10^{-3.5}$ atm) seem to have been equilibrated with the atmosphere (Appelo and Postma, 2010), which points to a larger contact time with the atmosphere and more stagnant conditions, as the water is not replenished by groundwater or drain inputs. Moreover, these boezem waters show an abundance of water plants and oxygen producing submerged plants (SI 3, photos Location B and Location B′).

We attribute the increase in variability, the increase of O_2 concentrations, and the apparent dilution of Cl and HCO_3 in the main ditches to be the result of the activation of the separate runoff collecting system in the polder during wet conditions. During the runoff events, the water that resided in the ditches is diluted by the runoff flux, which is high in O_2 (see Section 3.1). Under dry conditions the concentrations tend to be less variable and to be specifically enriched in Cl and HCO_3, reflecting the seepage of groundwater (groups 1 and 2, in Section 3.1).

3.2.2. Spatial variations in the groundwater composition affecting the surface water

Groundwater is affecting the water quality in the polder, leading to a substantial flux of anoxic water with high nutrient concentrations of NH_4 and TP (see also Fig. 3). In this section we explore how spatial differences in groundwater inputs may affect the surface water in our polder catchment. Table 1 summarizes the groundwater composition and reveals significant spatial variations in the groundwater influx. It is clear that both the shallow and deep groundwater contain significant concentrations of Cl, especially in the southern (GWS 1, 6, 7 and 8) and middle (GWS2) parts of the polder. Ammonium concentrations are significant, showing 20–50 mg/L NH_4 in deeper groundwater, and concentrations > 10 mg/L in the shallow groundwater wells that shows signs of brackish influence.

Table 1
Groundwater sampling results of two campaigns in May and November 2017.

	Campaign 2017-05-28				Campaign 2017-11-28			
	Cl	EC	$\delta^{13}C$-DIC	pCO_2	Cl	EC	NH_4	pCO_2
	mg/L	µS/cm	‰ VDPB	atm	mg/L	µS/cm	mg/L	atm
Shallow groundwater								
GWS1	496	2610	3.82	−1.36	483	2640	17.4	−1.27
GWS2	203	1660	−7.50	−0.97	187	1608	14.4	−0.99
GWS3		692	−8.00	−1.17	31	733	6.5	−1.07
GWS5	73	1338	−1.34	−0.90	55	1090	15.0	−0.85
GWS6	270	2180	3.09	−0.92	255	2138	19.5	−0.86
GWS7	211	2092	5.75	−1.06	15	516	2.8	−1.83
GWS8	285	2520	−3.66	−0.77	73	989	8.9	−1.18
Deeper groundwater								
GWD1	793	2515	8.17	−1.33	313	2048	20.5	−1.18
GWD2		3470			365	3300	49.6	−0.62
GWD3					243	2400	50.6	−0.85

Our data suggests that the hydrogeological build-up of the area is responsible for these spatial variations in both groundwater and surface water chemistry over the polder. Fig. 6 illustrates this hypothesis and provides a conceptual model for the differences observed. Our model suggests that the east ditches are fed by groundwater that has infiltrated in the adjacent boezem and in the upstream urban area east of the polder where a higher water level is maintained (right side of the cross-section). This dike seepage and shallow groundwater seepage would explain the lower Cl concentrations as the water is not replenished by the deeper groundwater in the first aquifer but follows a shallower flow path through the Holocene deposits, presumably at a level above the basal peat layer (Fig. 6). The relatively high pCO_2, HCO_3, and high ^{222}Rn of the water that seeps at the base of the dike at locations E1 and E2 implies a recent contact with the subsurface sediments and a typical groundwater origin.

However, especially the surface water in the SW corner of the polder catchment is affected by upward seepage of deeper groundwater with higher Cl concentrations. As the deeper groundwater has a higher hydraulic head than the managed water level in the main ditches M and W, an upward flow is maintained, that profits from the connection between the deeper aquifers and the shallow subsurface that once was established by the sandy tidal paleochannel. The fine sands that distinguish this channel have created a low resistance flow path (Fig. 6) that allows seepage from the deeper subsurface to enter the ditches. This mechanism is suggested to be the main cause of the high and temporally constant concentrations in the main ditches under dry conditions (Fig. 5).

Interestingly, also the δ^{13}C-DIC signature shows a trend over the shallow groundwater in the polder, showing very high δ^{13}C-DIC values in the wells GWS 1, 6 and 7 (all above 0) which corresponds with the high δ^{13}C-DIC of the deeper groundwater (GWD 1: δ^{13}C-DIC = 8.2‰ VDPB). This confirms the connection between the deeper groundwater and the shallow groundwater in this part of the polder (Fig. 6). A similar finding is recorded for the NH_4 concentrations. The shallower wells of GWS 1, 2 and 6 show high NH_4, resembling the 20 mg/L found in the deeper groundwater (see also SI, Section 5). Together, the high δ^{13}C-DIC, pCO_2 and NH_4 concentrations indicate that the process of methanogenesis has occurred in the deeper subsurface. Subsurface methanogenesis tends to enrich the remaining δ^{13}C of Dissolved Inorganic Carbon (e.g. Han et al., 2012), to increase the CO_2 partial pressure, and to mobilize nutrients N and P (see also Yu et al., 2018 who describe this for the larger Amsterdam region). In contrast, the shallow wells GWS 2, 3, 5 in the middle and northeast part of the polder show negative δ^{13}C-DIC, which excludes deeper groundwater feeding into the shallow groundwater in these parts of the polder (Fig. 6).

3.2.3. Water-atmosphere gas exchange

The analysis of spatial and temporal patterns of water quality in the urban polder reveals that runoff and rain flow during wet periods mixes with seeping groundwater. As the solutes reside in the surface water and are only slowly removed by pumping, atmospheric exchange may further determine the gases in solution leading to further changes in water chemistry. The PCA analysis (Section 3.1) indicates that concentrations of group 3 indicators, including pCO_2, ^{222}Rn, Fe and TP are lower than could be expected from the concentrations in the seeping groundwater. As shown in Section 3.1, indications exist that Fe and TP have been fixed by redox reactions involving O_2 and subsequent mineral precipitation and sorption. For pCO_2 and ^{222}Rn, the mechanism might be related to atmospheric exchange of CO_2 and radon gas, thus equilibrating with the concentrations and isotope ratios in the atmosphere. This process may promote the aeration of the surface water as degassing of CO_2 may coincide with the equilibration oxygen and the resulting uptake in the water column.

Indications for degassing of CO_2 and radon are indeed present in our polder system (Fig. 7) disclosing a clear relation of decreasing ^{222}Rn coupled to decreasing partial CO_2 pressure, for all 4 APEI classes. Here,

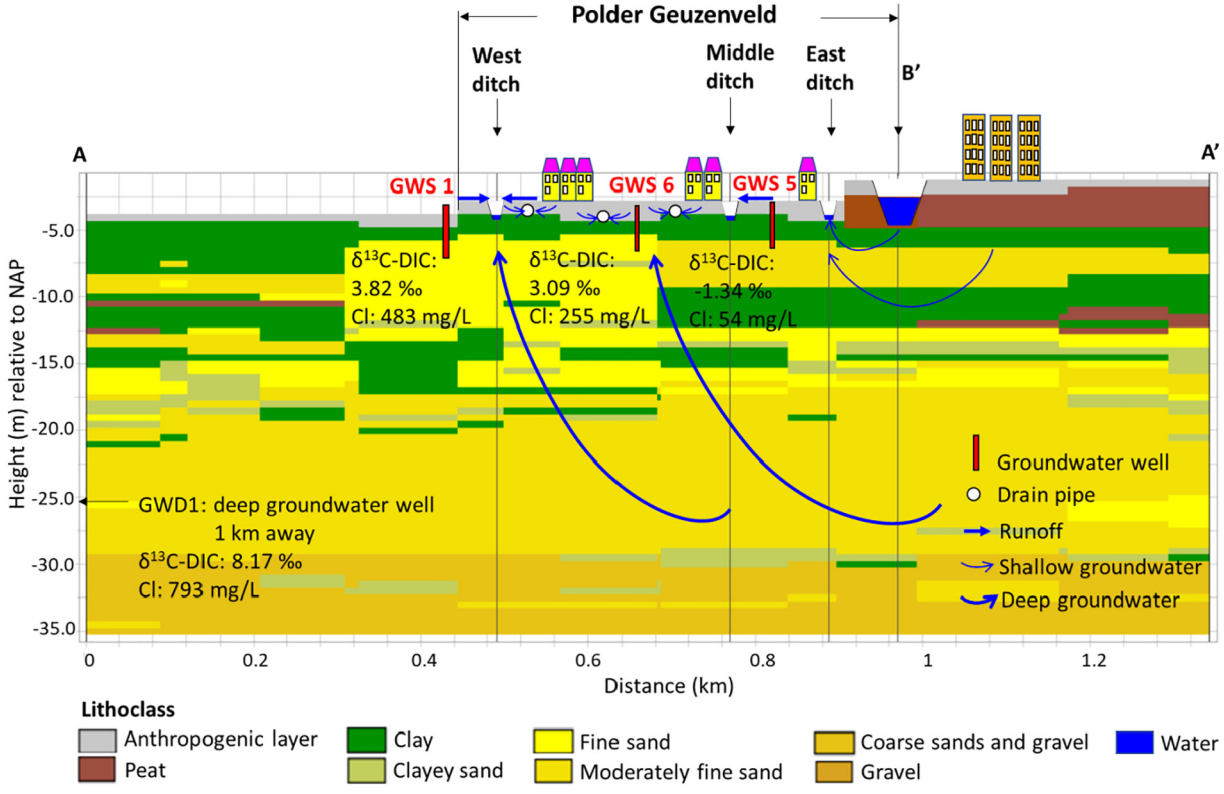

Fig. 6. Interpreted flow routes along the SW-NE cross-section showing the most probable lithology as provided by geostatistical characterization in GeoTOP (Schokker et al., 2015) and the water levels that are maintained in the waterways. Cl and δ^{13}C-DIC data are shown for a number of shallow groundwater observation wells and the deeper groundwater sampled 1 km SW of the polder.

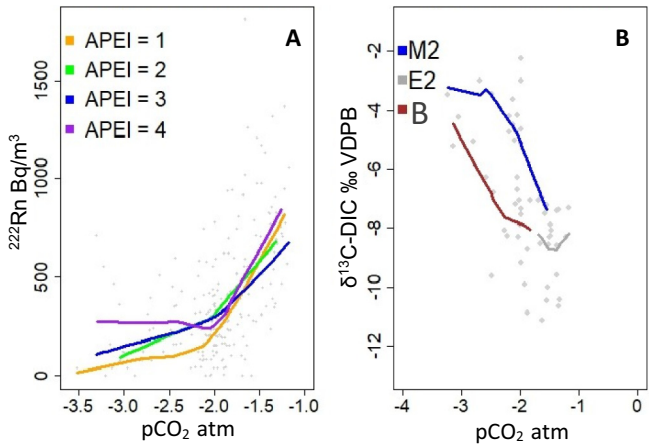

Fig. 7. Relations between ^{222}Rn, δ^{13}C-DIC and pCO_2 during the 2016–2017 monitoring campaign. A: ^{222}Rn versus pCO_2 for all 9 locations and divided over 4 APEI classes (1 = dry, 4 = most wet, LOWESS smooth represent the central tendency in the scatter), B: δ^{13}C-DIC versus pCO_2 for the location B, M2 and E2. LOWESS trend lines (Cleveland, 1979) were used to identify patterns in the scatter plots.

pCO_2 values of $10^{-1.5}$ atm point to typical groundwater pressures and $10^{-3.5}$ atm is representative for complete equilibrium with atmospheric CO_2 (Appelo and Postma, 2010; Mook, 2006). The data suggest that both ^{222}Rn and pCO_2 equilibrate with the atmosphere through gas exchange, which points to a significant residence time of water in the polder that also allows the slow aeration of the water in the gas exchange process. Equilibration of CO_2 and degassing and decay of ^{222}Rn seem to go hand-in-hand. Because the pattern exists for all APEI classes, we believe that the residence time of the water in the polder is such that there is ample time for degassing of CO_2 and radon and decay of radon in the surface water system under almost all weather conditions.

The δ^{13}C-DIC data give extra clues for this hypothesis (Fig. 7B). The δ^{13}C-DIC values measured at three locations in and outside the polder follow an inverse relation with the partial CO_2 pressure for locations B and M2. The δ^{13}C-DIC values are highest under conditions of CO_2 equilibrium with the atmosphere ($pCO_2 \sim 10^{-3.5}$) and lowest when typical groundwater partial CO_2 pressures are measured ($10^{-1.5}$ atm). This suggests that δ^{13}C fractionates during exchange with the atmosphere, leaving the remaining water in the ditch enriched in δ^{13}C following a Rayleigh type process (Mook, 2006). We relate the absence of such an exchange pattern in the shallow ditch E to the short residence time of water, which is confirmed by the high ^{222}Rn and partial CO_2 pressures in this ditch and the observation that the water flows significantly in this shallow ditch. For this interpretation, we need to assume that biological processes, such as primary production, play no role, which seems reasonable given the mere absence of water plants in the polder, combined with the low O_2 concentrations that were measured under dry conditions. These low O_2 conditions, that result from the continuous seepage of low-oxygen water to the polder water system, are assumed to be the prime reason for this lack of vegetation.

3.3. Temporal variations at the polder's main outlet

Further information about the functioning of the polder system was derived from studying the temporal patterns of the main solutes concentrations at the pumping location P, which covers the longest monitoring record. Fig. 8 shows the concentration ranges of the measured variables at location P in relation to the wetness classes from the APEI analysis (very dry (class 1), dry (2), wet (3) and very wet (4)) as done previously by Rozemeijer and Broers (2007). The graphs of Fig. 8

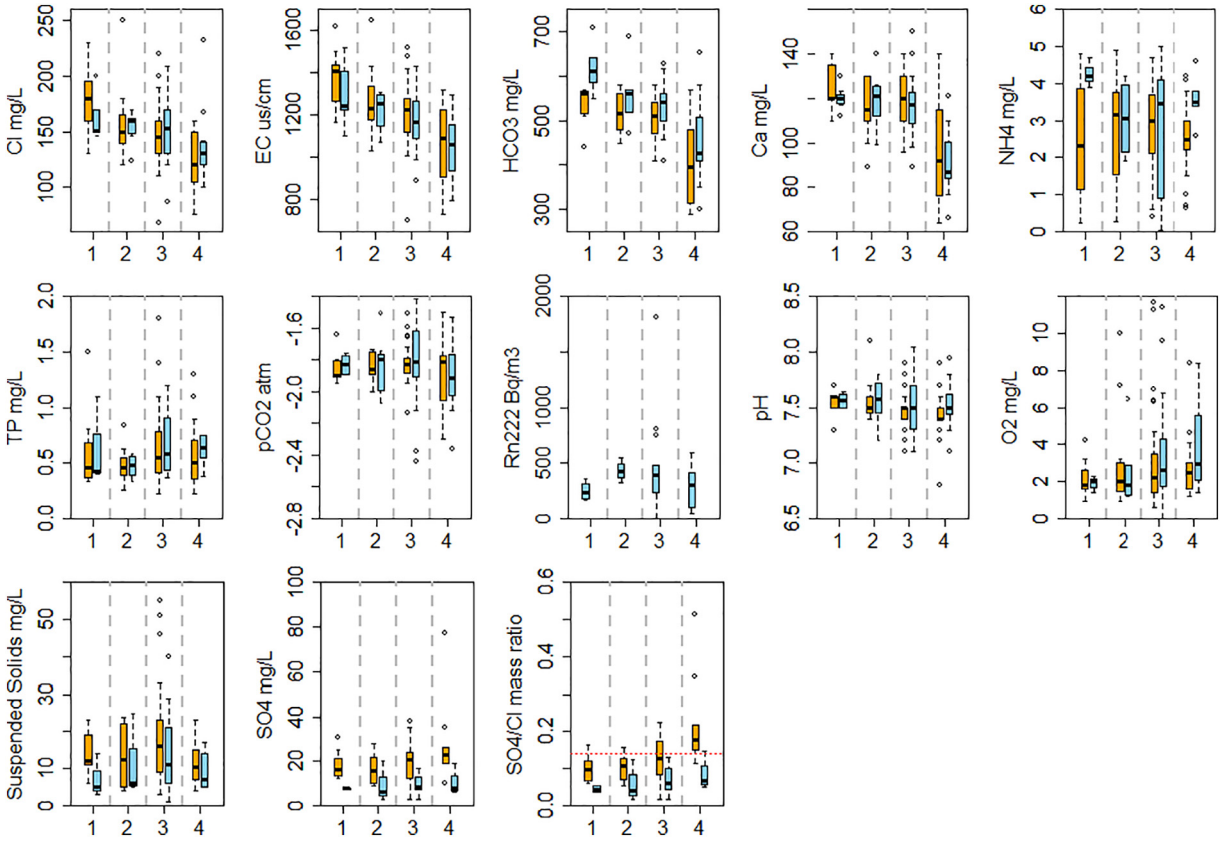

Fig. 8. Water quality at the main outlet as a function of catchment wetness (APEI classes 1 to 4, very dry to very wet). Orange: 2006–2016 long time series, blue: monitoring campaign 2016–2017. Red dash line indicates in SO_4/Cl 0.14.

combine the data of the long time series (2006–2016) and the March 2016–June 2017 monitoring campaign.

In general, the 2016–2017 weekly/biweekly dataset aligns well with the longer time series covering the monthly data of 2006–2017. A clear decreasing trend in concentrations from dry to wet conditions was observed for Cl, EC, HCO_3, and Ca, reflecting groups 1 and 2 of the PCA analysis (see Section 3.1). The opposite is true for the O_2 concentrations and the SO_4/Cl ratio (groups 4 and 6). Less distinct patterns occur for pH and pCO_2 (small decrease towards wetter conditions) and NH_4 (small decrease towards wet conditions but large variation). No significant pattern was observed for TP and suspended solids. The pattern for ^{222}Rn is deviant, showing the highest concentrations under intermediate wetness, and lower concentrations at very dry and very wet conditions.

The general trend observed for the main constituents of the water (Cl, HCO_3, Ca and EC, groups 1 and 2 of the PCA analysis) is a concentration decrease towards wetter conditions. This trend should be regarded as a dilution process, as runoff water is transported to the main water courses draining the polder and pumped out at the monitoring location. The increase in O_2 concentrations towards wetter conditions confirms this hypothesis, as the runoff was high in O_2 during the spatial survey under wet conditions as well (see Section 3.1). The smaller, less distinct decrease in NH_4 and TN (not shown) is probably also related to this dilution pattern. However, the temporal patterns of these nutrients may be obscured by the increased flow through the drain system which brings a mixture of rain water and shallow groundwater towards the main ditches. This drain water is now known to transport 3–5 mg/L of NH_4 which might effectively buffer the variability in NH_4 concentrations at the pumping station where all water is collected. This process might also be responsible for the decreasing trend in pH and the buffering of the partial CO_2 pressure going from dry to wet conditions.

Both drain flow and runoff may add to the increasing SO_4/Cl ratio. This ratio is an indicator of sulfate reduction which commonly occurs in the subsurface of this coastal area (Yu et al., 2018). SO_4/Cl ratios lower than 0.14 indicate subsurface sulfate reduction, and SO_4/Cl ratios above 0.14 indicates influence of additional SO_4 sources (Appelo and Postma, 2010; Griffioen et al., 2013; Yu et al., 2018). The boxplot pattern indicates that sulfate-reduced water with a SO4/Cl ratio < 0.14, which originated from groundwater seepage, is replaced and diluted with runoff and drain water that both carry SO_4 towards the main waterways in the polder (Fig. 4, and Group 6 in Fig. 3). Under the wettest conditions the long time series exceeds the 0.14 SO_4/Cl ratio indicating the discharge of drainage water carrying SO_4 presumably formed by pyrite oxidation (see before). It is no surprise that TP, pCO_2 and ^{222}Rn do not show the overall dilution patterns, as these variables were grouped together in the reactive group 3; solutes and gases that are supplied by groundwater but react or exchange within the polder system itself.

Here, the ^{222}Rn pattern of Fig. 8 seems most complicated. As a tracer of groundwater, the emanated ^{222}Rn is taken up by the groundwater when passing through soils and sediments (Grolander, 2009). We observed that ^{222}Rn was high in both shallow and deep groundwater (1500–4000 Bq/m^3, Fig. 5). At first sight, one would expect base flow to be traced by high ^{222}Rn concentrations from groundwater seepage, and therefore expect the highest ^{222}Rn at dry conditions. However, the residence time of ^{222}Rn in the surface water system is probably the longest under dry conditions with low surface water flows. Given the short half life time of dissolved ^{222}Rn of 3.8 days, ^{222}Rn in water that is no longer in contact with sediments will decrease relatively fast by both decay and exchange with the atmosphere which apparently led to concentrations < 350 Bq/m^3 in the ditch water under dry conditions. The highest ^{222}Rn concentrations at the pumping station were found at intermediate conditions between dry and wet (APEI classes 2 and 3, Fig. 5) where an optimum is obtained between the groundwater seepage and drain water fluxes (Fig. 4) that supply ^{222}Rn and the loss of ^{222}Rn through radioactive decay and atmospheric exchange. Under very wet conditions, the ^{222}Rn concentrations seem to be diluted by the influx of ^{222}Rn free runoff water, which explains the deviant ^{222}Rn pattern shown in Fig. 8.

3.4. The effects of urbanization on polder hydrogeochemistry

In the Netherlands and other lowland areas, expanding cities rely on areas that are not automatically optimal for urban development. Reclamation of wet areas, creating polder systems, requires the lowering of water levels and drainage of the areas. These polder systems demand a system for continuously pumping the surplus of seeping groundwater to higher grounds. The low water levels that are maintained enhance the oxidation of peat and pyrite and compaction of clay, which may release nutrients and heavy metals into shallow groundwater and the seepage of deeper nutrient-rich groundwater may amplify that problem as we disclosed in the paper. This study shows the strong effect that city infrastructure has on the reactive interfaces between O_2-rich rainwater and reduced deep groundwater. Our polder Geuzenveld is a lowland urban polder fed by a large amount of groundwater through four seasons. It has a separated drainage system that collects O_2-rich rain water and transports this into the ditches. The groundwater drainage system and the system of ditches effectively drain the area and a pumping station controls the surface water level in the polder. These infrastructures cause faster and shorter transport routes of groundwater into the open water system. The O_2-rich and heavy metals loaded runoff mixes with the anoxic, nutrient- and Fe-rich groundwater in the open ditch water system, leading to a number of subsequent hydrochemical processes in the polder, such as the precipitation of Fe-hydroxides, the sorption of phosphorus and exchange of gases with the atmosphere.

In lowland cities, the construction of separate drainage systems for runoff and shallow groundwater effectively changes the natural reactive interface between anoxic groundwater and oxic infiltrating water, bypassing the soil system that normally plays an attenuating role. Without a drainage system, part of the mixing and reactions are likely to take place in the redox transition zone within the soil or shallow subsurface and fluxes of Fe, As, P, and heavy metals may be attenuated. By separating the flow routes, both the nutrient-rich groundwater and the heavy metal rich runoff bypass the natural redox transition zone and directly enter the surface water system. The binding of P and heavy metals may then take place within the surface water system, but a larger proportion of the contaminants and metals may be able to affect downstream water resources.

In our urban system, the nutrient-rich groundwater and the oxygen- and metal-rich runoff bypass the soil system and mix only within the receiving ditch system, which yields a relatively dynamic water quality pattern with oxygen-low and oxygen-high phases alternating with time. Therefore, a side-effect of the separated flow routes is that the continuous supply of low-oxygen groundwater in dry periods seems to prevent the growth of water plants, leaving runoff and exchange of O_2 with the atmosphere as primary sources of O_2, thus determining the ecological status of the water system. Urbanizing wet lowlands and lowering water levels below sea level like in Geuzenveld inherently creates situations that are not easily manageable from a water quality perspective. Options for optimizing comparable urban groundwater-fed lowland catchments include actions to differently regulate water levels or measures to enhance the exchange between water bodies and/or the atmosphere. In our example, increasing surface water levels would somewhat reduce the seepage rate and the flux of anoxic, nutrient-rich, and brackish groundwater. However, the options are limited as groundwater levels in winter already reach the top 60 cm of the soil, and climate resilient water management also requires storage capacity in the subsurface and surface water system to cope with extremely wet periods. Sealing off the main ditches by clayey sediment barriers would be another option to reduce seepage but might increase the fluxes through the drainage system and raise water levels below the buildings. Remediation measures that enhance the exchange of water and gases would include to artificially increase O_2 concentrations in

dry periods, for example by flushing the polder system with inlet water from the oxygen-rich "boezem" system, or by enhancing the oxygen-mixing by promoting gas exchange with the atmosphere by artificial aeration and the creation of fountains. Further research is necessary on how to optimize artificial urban systems to deliver a better ecological and chemical status of the surface water. Such research should include a cost-benefit analysis of possible management strategies.

4. Conclusions

In this study, we identified the major flow routes of nutrients, heavy metals and major ions in a groundwater-influenced urban catchment and interpreted the mixing of the runoff, drain water, and groundwater in the surface water system through space and time. For this goal, we conducted a spatial and temporal analysis of water quality and isotope data using a 10-year dataset with monthly data and a monitoring campaign with a (bi)weekly frequency during the years 2016–2017.

In our urban lowland polder catchment, groundwater seepage constantly determines the surface water quality, being the main source of solutes in the water system. A Holocene tidal channel with sandy deposits in the SW of the polder hydraulically connects the deeper aquifer system with the shallow groundwater, thus providing a pathway for seepage of the high DIC and nutrient-rich waters present at 30 m depth. The resulting groundwater seepage is low in O_2 and high in Cl and the nutrients N and P. Runoff from the paved areas and roofs under wet weather conditions supplies the surface water system with O_2 and the trace metals Al, Cu, Pb, Zn, and Cd, and dilutes the water for all other components under wet weather conditions. PCA analysis reveals that mixing between these two flow components with contrasting chemistry is determining the composition of the water that is pumped from the catchment. An artificial groundwater drainage system provides a third flow route that captures a mixture of shallow groundwater and recently infiltrated rain water and adds to the sulfate concentrations and nutrients under intermediate and wet conditions. The PCA analysis helped to distinguish 6 subgroups of water quality variables that are indicative of the retention and reactivity of the different solutes in the open water system.

The concentrations that are pumped out at the polder outlet are a mixture of these transport routes and feed the receiving boezem water system with a time changing pattern of solutes. For the major groundwater derived solutes such as Cl, HCO_3, Ca, and Na, a clear dilution pattern in periods with low-mineralized runoff is obvious at the pump location. Other solutes, including Fe, TP, NH_4, pCO_2 and ^{222}Rn undergo retention and/or reactive processes. The data suggests (1) that TP is sorbed and fixated to Fe-hydroxides in the ditch sediments due to the mixing of oxygen-rich runoff with seeping groundwater, (2) that NH_4 is partly released from the shallow subsurface and (3) that CO_2 and ^{222}Rn undergo atmospheric exchange and/or radioactive decay, suggesting that the residence times of the water in the polder suffices to equilibrate the concentrations with the atmosphere, except under very wet conditions.

The regular low O_2 conditions in the water system of the polder, that result from the continuous supply of low-oxygen groundwater, seem to prevent aquatic plants growing there and leaves runoff and exchange of O_2 with the atmosphere as primary source of O_2, thus determining the ecological status of the water system. The separation of flow routes that is artificially created during the building of the residential area distinguishes the water quality processes from natural or agriculture dominated catchments. In our urban system, the nutrient-rich groundwater and the oxygen- and heavy/trace metal-rich runoff bypass the soil system and mix only within the receiving ditch system, which yields a relatively dynamic water quality pattern with oxygen-low and oxygen-high phases alternating with time. Further research is necessary on how to optimize artificial urban systems to deliver a better ecological and chemical status of the surface water.

Acknowledgements

This work was funded through China Scholarship Council (no. 201309110088) and supported by Waternet, the Strategic Research Funding of TNO and Deltares. We highly appreciate the help and support of the Waternet co-workers: Eelco Wiebenga, Henk Molenaar, Sonja Viester, Laura Moria, and Frank Smits. We thank Suzanne Verdegaal from the VU University Amsterdam for analyzing the $\delta^{13}C$-DIC samples.

Appendix A. Supplementary data

Supplementary data to this article can be found online at https://doi.org/10.1016/j.scitotenv.2019.04.428.

References

Abdalla, F., Khalil, R., 2018. Potential effects of groundwater and surface water contamination in an urban area, Qus City, Upper Egypt. J. Afr. Earth Sci. 141, 164–178.
Appelo, C.A.J., Postma, D., 2010. Geochemistry, Groundwater and Pollution. 2nd edition. CRC Press, UK.
Berndtsson, J.C., 2014. Storm water quality of first flush urban runoff in relation to different traffic characteristics. Urban Water J. 11 (4), 284–296.
Bonneau, J., Fletcher, T.D., Costelloe, J.F., Burns, M.J., 2017. Stromwater infiltration and the 'urban karst' — a review. J. Hydrol. 552, 141–150.
Boogaard, F.C., van de Ven, F., Langeveld, J.G., van de Giesen, N., 2014. Stormwater quality characteristics in (Dutch) urban area and performance of settlement basins. Challenges 5, 112–122.
Cartwright, I., Hofmann, H., 2016. Using radon to understand parafluvial flows and the changing locations of groundwater inflows in the Avon River, southeast Australia. Hydrol. Earth Syst. Sci. 20, 3581–3600.
Cecil, L.D., Green, J.R., 2000. Radon-222. In: Cook, P.G., Herczeg, A.L. (Eds.), Environmental Tracers in Subsurface Hydrology. Kluwer, Boston, USA, pp. 175–194.
Cleveland, W.S., 1979. Robust locally weighted regression and smoothing scatterplots. J. Am. Stat. Assoc. 74 (368), 829–836. https://doi.org/10.2307/2286407.
Delsman, J.R., Huang, K., Vos, P.C., de Louw, P.G.B., Oude Essink, G.H.P., Stuijfzand, P.J., Bierkens, M.F.P., 2014. Palaeo-modeling of coastal salt water intrusion during the Holocene: an application to the Netherlands. Hydrol. Earth Syst. Sci. 18, 3891–3905. https://doi.org/10.5194/hess-18-3891-2014.
Dent, D.L., Pons, L.J., 1995. A world perspective on acid sulphate soils. Geoderma 67, 263–276.
Dimova, N.T., Burnett, W.C., Chanton, J.P., Corbett, J.E., 2013. Application of Radon-222 to investigate groundwater discharge into small shallow lake. J. Hydrol. 486, 112–122.
EC, 2000. Council Directive of 23 October 2000 establishing a framework for Community action in the field of water policy. European Commission, Brussel.
Ellis, P.A., Rivett, M.O., 2007. Assessing the impact of VOC-contaminated groundwater on surface water at the city scale. J. Contam. Hydrol. 91, 107–127.
Foster, S.S.D., 2001. The interdependence of groundwater and urbanization in rapidly developing cities. Urban Water 185–192.
Gabor, R.S., Hall, S.J., Eiriksson, D.P., Jameel, Y., Millington, M., Stout, T., Barnes, M.L., Gelderloos, A., Tennant, H., Bowen, G.J., Neilson, B.T., Brooks, P.D., 2017. Persistent urban influence on surface water quality via impacted groundwater. Environ. Sci. Technol. 51, 9477–9487.
Galan, I., Andrade, C., Mora, P., Sanjuan, M.A., 2010. Sequestration of CO_2 by concrete carbonation. Environ. Sci. Technol. 44, 3181–3186.
Gobel, P., Dierkes, C., Coldewey, W.G., 2007. Storm water runoff concentration matrix for urban areas. J. Contam. Hydrol. 91, 26–42.
Griffioen, J., Vermooten, S., Janssen, G., 2013. Geochemical and palaeohydrological controls on the composition of shallow groundwater in the Netherlands. Appl. Geochem. 39, 129–149.
Grolander, S., 2009. Radon as a groundwater tracer in Forsmark and Laxemar. SKB Rapport R-09-47 ISSN 1402-3091.
Gumindoga, W., Rientjes, T., Shekede, M.D., Rwasoka, D.T., Nhapi, I., Haile, A.T., 2014. Hydrological impacts of urbanization of two catchments in Harare, Zimbabwe. Remote Sens. 6 (12), 12544–12574.
Hall, M.J., Ellis, J.B., 1985. Water quality problems of urban areas. GeoJournal 11 (3), 265–275.
Han, L. F., Plummer, L. N., Aggarwal, P.: A graphical method to evaluate predominant geochemical processes occurring in groundwater systems for radiocarbon dating. Chem. Geol., 318–319: 88–112, 2012. doi.org/https://doi.org/10.1016/j.chemgeo.2012.05.004.
Hobbie, S. E., Finlay, J. C., Janke, B. D., Nidzgorski, D. A., Millet, D. B., Baker, L.A.: Contrasting nitrogen and phosphorus budgets in urban watersheds and implications for managing urban water pollution. PNAS, 114(16): 4177–4182, 2017. doi.org/https://doi.org/10.1073/pnas.1618536114.
Howard, K.W.F., Maier, H., 2007. Road de-icing salt as a potential constraint on urban growth in the Greater Toronto Area, Canada. J. Contam. Hydrol. 91 (1–2), 146–170.
Kojima, K., Sano, S., Kurisu, F., Furumai, H., 2017. Estimation of source contribution to nitrate loading in road runoff using stable isotope analysis. Urban Water J. 14, 337–342.
Leopold, L.B., 1968. Hydrology for Urban Land Planning-A Guidebook on the Hydrologic Effects of Urban Land Use. U.S. Geological Survey, Washington, D.C.

Makkink, G.F., 1957. Testing the Penman formula by means of lysimeters. J. Inst. Water Eng. Sci. 11, 277–288.
McPherson, M.B., 1974. Hydrological Effects of Urbanization. Report of the Sub-group on the Effects of Urbanization on the Hydrological Environment, of the Co-ordinating Council of the International Hydrological Decade. The Unesco Press, Paris.
Mook, W.G., 2006. Introduction to isotope hydrology: stable and radioactive isotopes of hydrogen, oxygen and carbon. IAH International Contributions to Hydrogeology. vol. 25. Taylor & Francis, London New York. ISBN: 9780415381970, p. 226.
Morris, B.L., Darling, W.G., Cronin, A.A., Rueedi, J., Whitehead, E.J., Gooddy, D.C., 2006a. Assessing the impact of modern recharge on a sandstone aquifer beneath a suburb of Doncaster, UK. Hydrogeol. J. 14, 979–997.
Morris, B.L., Darling, W.G., Gooddy, D.C., Litvak, R.G., Neumann, I., Nemaltseva, E.J., Podubnaia, I., 2006b. Assessing the extent of induced leakage to an urban aquifer using environmental tracers: an example from Kyrgyzstan, Central Asia. Hydrogeol. J. 14 (1–2), 225–243.
NAP, d. https://nl.wikipedia.org/wiki/Normaal_Amsterdams_Peil (2019-02-12).
Nyenje, P.M., Foppen, J.W., Uhlenbrook, S., Kulabako, R.N., Muwanga, A., 2010. Eutrophication and nutrient release in urban areas of sub-Saharan Africa-a review. Sci. Total Environ. 408 (3), 447–455.
Oros, D.R., Ross, J.R.M., Spies, R.B., Mumley, T.E., 2007. Polycyclic aromatic hydrocarbon (PAH) contamination in San Francisco Bay: a 10-year retrospective of monitoring in an urbanized estuary. Environ. Res. 105, 101–118.
Pataki, D.E., Boone, C.G., Hogue, T.S., Jenerette, G.D., McFadden, J.P., Pincetl, S., 2011. Ecohydrology bearings-invited commentary: socio-ecohydrology and the urban water challenge. Ecohydrology 4, 341–347. https://doi.org/10.1002/eco.209.
Paul, M.J., Meyer, J.L., 2001. Streams in the urban landscape. Annu. Rev. Ecol. Syst. 32, 333–365.
Rozemeijer, J.C., Broers, H.P., 2007. The groundwater contribution to surface water contamination in a region with intensive agricultural land use (Noor-Brabant, The Netherlands). Environ. Pollut. 148, 695–706.
Rozemeijer, J.C., van der Velde, Y., van Geer, F., de Rooij, G.H., Torfs, P.J.J.F., Broers, H.P., 2010. Improving load estimates for NO_3 and P in surface waters by characterizing the concentration response to rainfall events. Environ. Sci. Technol. 44 (16), 6305–6312.
Schokker, J., Bakker, M.A.J., Dubelaar, C.W., Dambrink, R.M., Harting, R., 2015. 3D subsurface modelling reveals the shallow geology of Amsterdam. Neth. J. Geosci. 94 (4), 399–417. https://doi.org/10.1017/njg.2015.22.
Smolders, E., Degryse, F., 2002. Fate and effect of zinc from tire debris in soil. Environ. Sci. Technol. 36 (17), 3706–3710.
Sorensen, J.P.R., Lapworth, D.J., Nkhuwa, D.C.W., Stuart, M.E., Gooddy, D.C., Bell, R.A., Chirwa, M., Kabika, J., Liemisa, M., Chibesa, M., Pedley, S., 2015. Emerging contaminants in urban groundwater sources in Africa. Water Res. 72, 51–63.
Stafleu, J., Maljers, D., Gunnink, J.L., Menkovic, A., Busschers, F.S., 2011. 3D modelling of the shallow subsurface of Zeeland, the Netherlands. Neth. J. Geosci. 90 (4), 293–310.
Van der Grift, B., Rozemeijer, J.C., Griffioen, J., van der Velde, Y., 2014. Iron oxidation kinetics and phosphate immobilization along the flow-path from groundwater into surface water. Hydrol. Earth Syst. Sci. 18, 4687–4702.
Van der Grift, B., Osté, L., Schot, P., Kratz, A., van Popta, E., Wassen, M., Griffioen, J., 2018. Forms of phosphorus in suspended particulate matter in agriculture-dominated lowland catchments: iron as phosphorus carrier. Sci. Total Environ. 631-632, 115–129.
Van der Sloot, et al., 2011. Enviromental Criteria for Cement Based Products. ECRICEM, ECN Report ECN-E-11-020. Petten, The Netherlands. .
Van Mourik, W., van der Mijle, M.H.J., van Tilborg, W.J.M., Teunissen, R.J.M., 2003. Emissies van bouwmaterialen. RIZA report 9036956412 https://doi.org/10.1021/es025567p 027. (in Dutch).
Walsh, C.J., Fletcher, T.D., Ladson, A.R., 2005. Stream restoration in urban catchments through redesigning stormwater systems: looking to the catchment to save the stream. J. N. Am. Benthol. Soc. 24 (3), 690–705.
Yan, R., Li, L., Gao, J., 2018. Modeling the regulation effects of lowland polder with pumping station on hydrological processes and phosphorus loads. Sci. Total Environ. 637-638, 200–207.
Yang, Y. Y. and Toor, G. S.: Stormwater runoff driven phosphorus transport in an urban residential catchment: implications for protecting water quality in urban watersheds. Nat. Sci. Rep. 2018(8): 11681. doi.org/https://doi.org/10.1038/s41598-018-29857-x.
Yu, L., Rozemeijer, J.C., van Breukelen, B.M., Ouboter, M., van der Vlugt, C., Broers, H.P., 2018. Groundwater impacts on surface water quality and nutrient loads in lowland polder catchments: monitoring the greater Amsterdam area. Hydrol. Earth Syst. Sci. 22, 487–508.
Zafra, C., Temprano, J., Tejero, I., 2017. The physical factors affecting heavy metals accumulated in the sediment deposited on road surfaces in dry weather: a review. Urban Water J. 14 (6), 639–649.
Zhang, Y.C., Slomp, C.P., Broers, H.P., Passier, H.F., Böttcher, M.E., van Cappellen, P., 2009. Sources and fate of nitrate and sulfate in a sandy aquifer: a multi-isotope study. Geochim. Cosmochim. Acta 73, A1513.